

An FDTD Formulation for Dispersive Media Using a Current Density

Qing Chen, Makoto Katsurai, and Paul H. Aoyagi

Abstract—A novel finite-difference time-domain (FDTD) formulation for dispersive media called the JE convolution (JEC) method is derived using the convolution relationship between the current density \mathbf{J} and the electric field \mathbf{E} . The high accuracy of the JEC method is confirmed by computing the reflection and transmission coefficients for a nonmagnetized plasma slab in one dimension. It is found that the new method has accuracy comparable to the auxiliary differential equation (ADE) while having the same computational efficiency as the less accurate recursive convolution (RC) method. Numerical simulations also show that the JEC method exhibits significantly higher accuracy than the RC method in modeling wave attenuation inside the plasma.

Index Terms—Dispersive media, FDTD methods.

I. INTRODUCTION

THE finite-difference time-domain (FDTD) method [1]–[4] has been widely used to calculate the electromagnetic fields associated with a variety of problems in electromagnetics such as antennas, waveguide propagation, and scattering. Recently, the FDTD method has also been extended to include computation of wave propagation in dispersive media. In the past, there have been numerous investigations of FDTD dispersive media formulations. These include the recursive convolution (RC) methods [5]–[13], the auxiliary differential equation (ADE) method [14]–[21], frequency-dependent Z transform [22], and a full FDTD method coupling equations of Maxwell and Euler [23]. Although possessing the lowest accuracy of all the methods mentioned, the original RC method (simply called the RC method in this paper) tends to be the most computationally efficient [13].

In this paper, a new finite-difference time-domain (FDTD) formulation, i.e., the JE convolution (JEC) method, to model electromagnetic wave propagations in dispersive media is derived using a convolution relationship between the current density of the media \mathbf{J} and the electric field \mathbf{E} . In particular, the \mathbf{J} at a future time step is computed from previous values of \mathbf{J} in conjunction with a convolution in time of previously computed values of \mathbf{E} . \mathbf{J} is, in turn, used with the FDTD algorithm to compute \mathbf{E} and the magnetic field \mathbf{H} at a future time step. For computational efficiency, the convolution is computed using a recursive update. Though closely related to the RC method [5], it is shown that the JEC method possesses

greater accuracy (especially for lossy plasmas) but retains the same computational efficiency. In Section II, we derive the JE convolution (JEC) formulation for a nonmagnetized plasma. In Section III, we examine the relationship between the JEC and the RC methods. In Section IV, we evaluate the accuracy of the JEC, ADE, and RC methods by performing numerical simulations to compute the reflection and transmission coefficients of a nonmagnetized plasma slab in one dimension. The factors affecting the result accuracy of the RC method will be also discussed in this section.

II. DERIVATION OF THE JEC METHOD FOR A NONMAGNETIZED PLASMA

Consider the kinetic equations for an isotropic nonmagnetized cold electron plasma driven by a small amplitude time-varying electric field [24]–[26], i.e.,

$$\nabla \times \mathbf{E} = -\mu_0 \frac{\partial \mathbf{H}}{\partial t} \quad (1)$$

$$\nabla \times \mathbf{H} = \epsilon_0 \frac{\partial \mathbf{E}}{\partial t} + \mathbf{J} \quad (2)$$

$$\mathbf{J} = -en_{e0}\mathbf{u}_e \quad (3)$$

$$\frac{\partial \mathbf{u}_e}{\partial t} = -\frac{e}{m_e} \mathbf{E} - \nu_c \mathbf{u}_e \quad (4)$$

where n_{e0} is the density of the electron at steady state, ν_c is the collision frequency, \mathbf{u}_e is the electron velocity, m_e is the electron mass, and e is the electron charge.

For a time-harmonic dependence, the following frequency-domain relationship between \mathbf{J} and \mathbf{E} can be derived from (3) and (4), i.e.,

$$\mathbf{J}(\omega) = \epsilon_0 \frac{\omega_{pe}^2}{j\omega + \nu_c} \mathbf{E}(\omega) = \sigma(\omega) \mathbf{E}(\omega) \quad (5)$$

where

$$\omega_{pe} = \left(\frac{e^2 n_{e0}}{\epsilon_0 m} \right)^{1/2} = \text{plasma frequency [rad/s]} \quad (6)$$

$$\sigma(\omega) = \epsilon_0 \frac{\omega_{pe}^2}{j\omega + \nu_c}. \quad (7)$$

Taking the inverse transform of (5) and (7), we obtain

$$\mathbf{J}(t) = \int_0^t \sigma(t-\tau) \mathbf{E}(\tau) d\tau = \epsilon_0 \omega_{pe}^2 e^{-\nu_c t} \int_0^t e^{\nu_c \tau} \mathbf{E}(\tau) d\tau \quad (8)$$

where

$$\sigma(t) = \epsilon_0 \omega_{pe}^2 e^{-\nu_c t} u(t) \quad (9)$$

and $u(t)$ is the unit step function.

Manuscript received October 22, 1996; revised April 25, 1997.
 Q. Chen and M. Katsurai are with the Department of Electrical Engineering, University of Tokyo, 113 Japan.
 P. H. Aoyagi is with the Production Engineering Research Laboratory, Hitachi, Ltd., Yokohama, 244 Japan.
 Publisher Item Identifier S 0018-926X(98)07493-6.

Equations (1), (2), and (8) are approximated in the JEC method. If we define \mathbf{E} is at integer time steps, i.e., E^n , while \mathbf{H} and \mathbf{J} at half integer time steps, i.e., $H^{n+1/2}$, and $J^{n+1/2}$, (1) and (2) can be readily integrated into the FDTD algorithm in a one-dimensional case

$$H_{z_{i+1/2}}^{n+1/2} = H_{z_{i+1/2}}^{n-1/2} - \frac{\Delta t}{\mu_0 \Delta x} (E_{y_{i+1}}^n - E_{y_i}^n) \quad (10)$$

$$E_{y_i}^{n+1} = E_{y_i}^n - \frac{\Delta t}{\varepsilon_0 \Delta x} (H_{z_{i+1/2}}^{n+1/2} - H_{z_{i-1/2}}^{n+1/2}) - \frac{\Delta t}{\varepsilon_0} J_{y_i}^{n+1/2}. \quad (11)$$

In discrete form for (8), we note that it can be written as

$$J_{y_i}^{n+1/2} = \varepsilon_0 \omega_{pe}^2 e^{-\nu_c(n+1/2)\Delta t} \int_0^{(n+1/2)\Delta t} e^{\nu_c \tau} E_{y_i}(\tau) d\tau. \quad (12)$$

By approximating the convolution integral in (12) using a discrete rectangular rule summation (see Appendix A), the following second-order approximation for \mathbf{J} at a future time step can be derived in explicit form

$$J_{y_i}^{n+1/2} = e^{-\nu_c \Delta t} J_{y_i}^{n-1/2} + \varepsilon_0 \omega_{pe}^2 e^{-\nu_c \Delta t/2} E_{y_i}^n \Delta t. \quad (13)$$

With regard to computational requirements, because $J_{y_i}^{n-1/2}$ is needed to compute $J_{y_i}^{n+1/2}$ at every time step, the JEC method requires one more storage in addition to the normal FDTD storage of the electromagnetic field components.

Derivations of the JEC formulation for two other types of dispersive media, i.e., Debye relaxation and Lorentzian resonance, are given in Appendixes B and C.

III. RELATIONSHIP BETWEEN THE JEC AND RC METHODS

To investigate the relationship between the JEC and RC methods, we consider the formulation for a nonmagnetized plasma. We begin by noting that the RC method is based on the following:

$$\nabla \times \mathbf{H} = \frac{\partial \mathbf{D}}{\partial t} \quad (14)$$

$$\begin{aligned} \mathbf{D}(t) &= \varepsilon(t) * \mathbf{E}(t) = \varepsilon_0 \mathbf{E}(t) + \varepsilon_0 \chi(t) * \mathbf{E}(t) \\ &= \varepsilon_0 \mathbf{E}(t) + \varepsilon_0 \int_0^t \chi(\tau) \mathbf{E}(t - \tau) d\tau \\ &= \varepsilon_0 \mathbf{E}(t) + \varepsilon_0 \frac{\omega_{pe}^2}{\nu_c} \int_0^t (1 - e^{-\nu_c \tau}) \mathbf{E}(t - \tau) d\tau \end{aligned} \quad (15)$$

where \mathbf{D} = electric flux density and

$$\varepsilon(t) = \varepsilon_0 \left[\delta(t) + \frac{\omega_{pe}^2}{\nu_c} (1 - e^{-\nu_c t}) u(t) \right] \quad (16)$$

$$\chi(t) = \frac{\omega_{pe}^2}{\nu_c} (1 - e^{-\nu_c t}) u(t). \quad (17)$$

By approximating (14) and (15) using central finite differencing of the space and time derivatives and a first-order rectangular rule approximation for the convolution integral the formulations in the RC method become

$$-\frac{H_{z_{i+1/2}}^{n+1/2} - H_{z_{i-1/2}}^{n+1/2}}{\Delta x} = \frac{D_{y_i}^{n+1} - D_{y_i}^n}{\Delta t} \quad (18)$$

$$D_{y_i}^{n+1} = \varepsilon_0 E_{y_i}^{n+1} + \varepsilon_0 \sum_{m=0}^n E_{y_i}^{n-m+1} \int_{m\Delta t}^{(m+1)\Delta t} \chi(\tau) d\tau. \quad (19)$$

A characteristic equation for the RC method, as shown in (20) at the bottom of the page, is derived by substituting (19) into (18).

The JEC method can be related to the RC method by slightly modifying one of the fundamental equations used in the RC method derivation. In particular, we can use the commutative property of the convolution to rewrite (15) as

$$\begin{aligned} \mathbf{D}(t) &= \varepsilon_0 \mathbf{E}(t) + \varepsilon_0 \int_0^t \chi(t - \tau) \mathbf{E}(\tau) d\tau \\ &= \varepsilon_0 \mathbf{E}(t) + \varepsilon_0 \frac{\omega_{pe}^2}{\nu_c} \int_0^t (1 - e^{-\nu_c(t-\tau)}) \mathbf{E}(\tau) d\tau. \end{aligned} \quad (21)$$

By using (21) rather than (15) an expression for $(\partial \mathbf{D}(t)/\partial t)$ can be readily obtained

$$\frac{\partial \mathbf{D}(t)}{\partial t} = \varepsilon_0 \frac{\partial \mathbf{E}(t)}{\partial t} + \varepsilon_0 \frac{\partial}{\partial t} [\chi(t) * \mathbf{E}(t)] \quad (22)$$

$$\begin{aligned} \frac{\partial \mathbf{D}}{\partial t} &= \varepsilon_0 \frac{\partial \mathbf{E}}{\partial t} + \frac{\varepsilon_0 \omega_{pe}^2}{\nu_c} \frac{\partial}{\partial t} \left[\int_0^t (1 - e^{-\nu_c(t-\tau)}) \mathbf{E}(\tau) d\tau \right] \\ &= \varepsilon_0 \frac{\partial \mathbf{E}}{\partial t} + \frac{\varepsilon_0 \omega_{pe}^2}{\nu_c} \frac{\partial}{\partial t} \\ &\quad \cdot \left[\int_0^t \mathbf{E}(\tau) d\tau - e^{-\nu_c t} \int_0^t e^{\nu_c \tau} \mathbf{E}(\tau) d\tau \right] \\ &= \varepsilon_0 \frac{\partial \mathbf{E}}{\partial t} + \varepsilon_0 \omega_{pe}^2 e^{-\nu_c t} \int_0^t e^{\nu_c \tau} \mathbf{E}(\tau) d\tau \end{aligned} \quad (23)$$

where the fundamental equation

$$\phi(x) = \int_a^x f(t) dt, \quad \text{then} \quad \phi(x) = f(x) \quad (24)$$

is used.

By substituting (23) into (14) we obtain the same fundamental equations used in the derivation of the JEC method given earlier in Section II:

$$\nabla \times \mathbf{H} = \frac{\partial \mathbf{D}}{\partial t} = \varepsilon_0 \frac{\partial \mathbf{E}}{\partial t} + \mathbf{J} \quad (25)$$

$$\mathbf{J} = \varepsilon_0 \omega_{pe}^2 e^{-\nu_c t} \int_0^t e^{\nu_c \tau} \mathbf{E}(\tau) d\tau. \quad (26)$$

$$-\frac{H_{z_{i+1/2}}^{n+1/2} - H_{z_{i-1/2}}^{n+1/2}}{\Delta x} = \frac{\varepsilon_0 E_{y_i}^{n+1} + \varepsilon_0 \sum_{m=0}^n E_{y_i}^{n-m+1} \int_{m\Delta t}^{(m+1)\Delta t} \chi(\tau) d\tau - \varepsilon_0 E_{y_i}^n - \varepsilon_0 \sum_{m=0}^{n-1} E_{y_i}^{n-m+1} \int_{m\Delta t}^{(m+1)\Delta t} \chi(\tau) d\tau}{\Delta t} \quad (20)$$

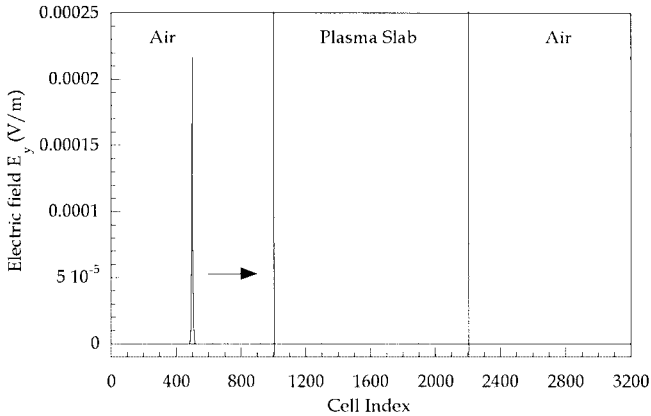


Fig. 1. Sample of electric field versus cell at the time step $120\Delta t$, $dx = 75 \mu\text{m}$, $dt = 0.125 \text{ ps}$.

By comparing the derivations given above, we note that there are two reasons why we would expect the RC method to be less accurate than the JEC method. The first reason is that the RC method contains an additional finite-difference approximation, i.e., that of $d\mathbf{D}/dt$, which is not contained in the JEC method. This difference can be traced to the fact that the convolution integral, i.e., (21), used in the derivation of the JEC method is in a form which allows the differentiation of \mathbf{D} to be readily carried out analytically. The second reason is that the RC method contains a first-order approximation to the convolution integral of \mathbf{D} in (19) caused by the rectangular-rule approximation. In contrast, it is shown in Appendix A that the rectangular rule approximation to the corresponding convolution integral contained in the JEC method is second-order in Δt . Despite the increased accuracy of its approximations, we note that the computational requirements for the JEC method (shown in the Section II) are the same as that of the RC method [5].

IV. NUMERICAL RESULTS

To investigate the accuracy of the JEC and RC methods we compute the frequency dependent reflection and transmission coefficients of a nonmagnetized plasma slab ($\omega_{pe} = 2\pi * 28.7 * 10^9 \text{ rad/s}$, $\nu_c = 20 * 10^9 \text{ rad/s}$) with a thickness of 9.00 cm (Fig. 1). This simulation is identical to that performed in [5] except the plasma slab is increased to better illustrate the effects of plasma attenuation. In addition, we also consider a simulation for $\nu_c = 2 * 10^9 \text{ rad/s}$. As a further comparison of the accuracy of each method, we also compute the same coefficients using the ADE method. The reflection and transmission coefficients were computed by simulating the transient response of a normally incident plane wave on the plasma slab. The incident wave used in the simulation is a Gaussian pulse whose frequency spectrum peaks at 50 GHz and is 10 dB down from the peak at 100 GHz. Fourier transform is used to compute the reflection and transmission coefficients of the plasma slab from the reflected and transmitted pulses at the air-to-plasma and plasma-to-air interfaces, respectively. The frequency range of computation was 0–80 GHz. The spatial discretization, Δx , used in the

simulations is $75 \mu\text{m}$ and the time step $\Delta t (= 0.5\Delta x/c)$ is 0.125 ps . Simulations were carried out over 15 000 Δt .

Figs. 2 and 3 compare the reflection and transmission coefficients computed using the JEC, ADE, and RC methods with those of the analytical solution for a plasma with $\nu_c = 2010^9 \text{ rad/s}$. Fig. 2(a) and (c) shows that the JEC and ADE methods are in agreement with the analytical solution for both the reflection coefficient magnitude and phase. We note that both methods accurately model the oscillatory behavior in the magnitudes at the high frequencies caused by the internal reflections within the slab. Likewise, Fig. 3(a) and (b) shows that the JEC and ADE methods are also in excellent agreement with the analytical transmission coefficient magnitude and phase. In contrast, Fig. 2(b) and (d) shows that the RC method is in good agreement with the analytical magnitude and phase when the reflection coefficient has a large magnitude but exhibits noticeable error for smaller magnitudes. With respect to the transmission coefficient, Fig. 3(a) shows that the RC method computations suffers from a relatively large error, i.e., $>2.5 \text{ dB}$, even for large values of the transmission coefficient (we note that because the transmission coefficient magnitude for frequencies less than about 28 GHz is $<-100 \text{ dB}$, this range is not shown). An explanation for why the RC method exhibits larger error in the transmission as opposed to the reflection coefficient computations can be given using a multiple reflection model, e.g., [27]. In particular, we note that the reflection coefficient is dominated by the first reflection off the plasma slab rather than the higher order reflections which arise from waves inside the plasma slab. In contrast, the dominant term for the transmission coefficient is a wave that has propagated once across the plasma slab. Consequently, the RC modeling errors of the plasma affect the accuracy of the transmission coefficient computation more than that of the reflection coefficient. Despite large errors in modeling the transmission magnitudes, however, we note that Fig. 3(b) shows that the RC method exhibits the same high accuracy as the JEC and ADE methods in modeling the phase of the transmission coefficient.

Figs. 4 and 5 show the magnitude and phase of the reflection and transmission coefficients computed using the JEC, ADE, and RC methods and the analytical solution for a plasma with $\nu_c = 210^9 \text{ rad/s}$. The choice of ν_c was made to reduce the attenuation in the plasma. Unlike the previous example, Figs. 4 and 5 show that the JEC, ADE, and RC methods are all in excellent agreement with the analytical reflection and transmission coefficients. These results illustrate that the RC method can have the same accuracy in practice as the JEC and ADE methods provided the losses associated with the propagation through the plasma are small. We note that in addition to decreasing ν_c , the loss through the nonmagnetized plasma can also be decreased by decreasing ω_{pe} and the slab thickness. Of interest, we note that the highly accurate RC method simulation results given in [5] were likely achieved through the use of thin plasma slabs. We conclude that the practical advantage of the JEC method over the RC method is that it provides a more accurate model for lossy plasma environments for the same computational efficiency, i.e., memory storage and operation count. Moreover, by noting

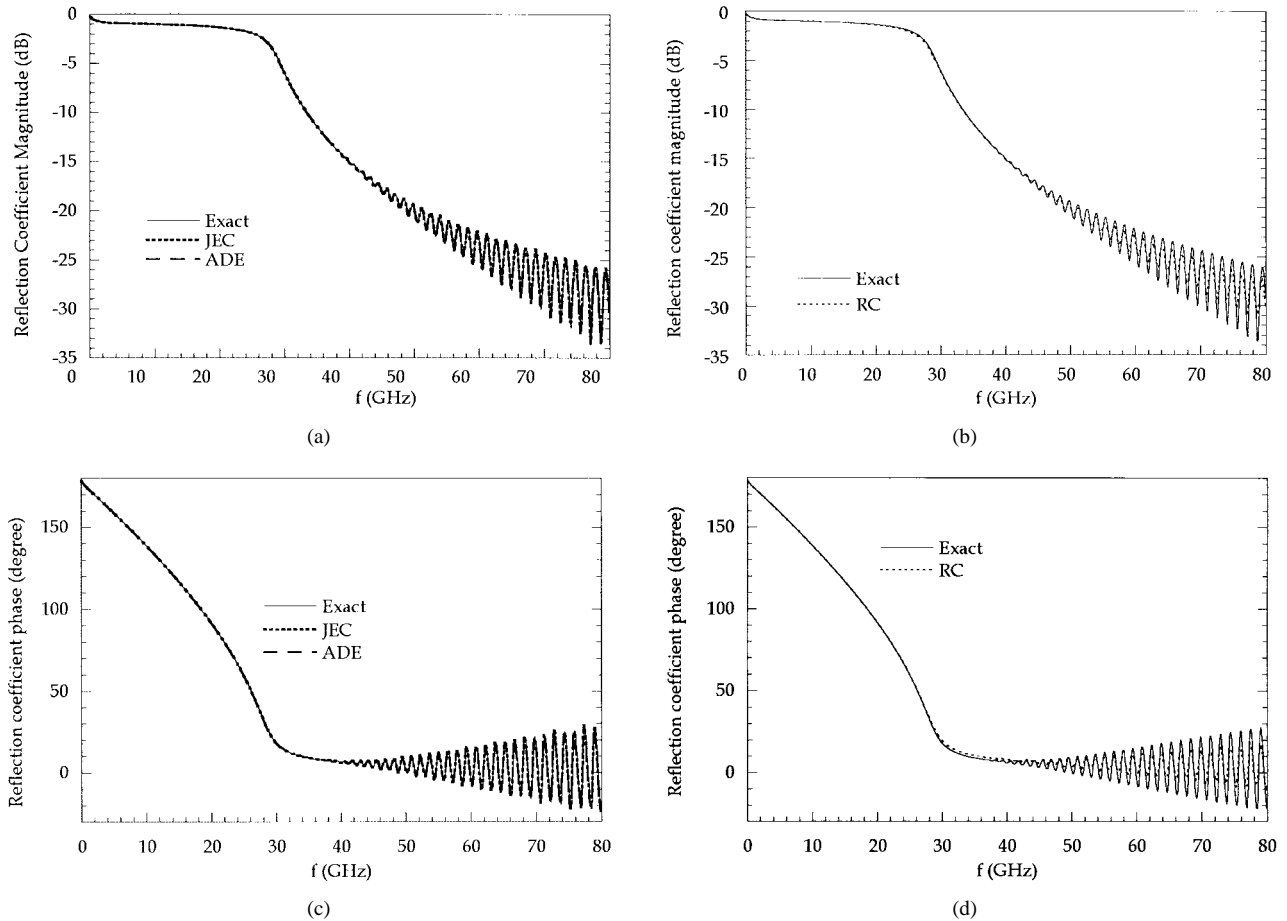


Fig. 2. Reflection coefficient magnitude for $V_c = 20 \times 10^9$ rad/m computed using (a) JEC and ADE methods, (b) RC method, (c) the reflection coefficient phase computed using the JEC and ADE methods, and (d) the RC method.

that the ADE method requires more computational memory than the RC method [13], [20], we can conclude that the JEC method requires less memory than the ADE method to achieve the same high accuracy.

V. CONCLUSION

In this paper, we introduced an FDTD formulation, i.e., the JEC method, for modeling dispersive medium based on the relationship of current density inside the media \mathbf{J} and electric field \mathbf{E} in dispersive media. In particular, JEC formulations for the cases of nonmagnetized plasmas, Debye relaxation, and Lorentzian resonance were given. The JEC method allows the differentiation $d\mathbf{D}/dt$ to be readily carried out analytically instead of using the central difference approximation for $d\mathbf{D}/dt$ in the RC method. This changes the upper time limit of the convolution term, and makes higher order accurate formulations in the JEC method. The high accuracy of the JEC method was confirmed by computing the reflection and transmission coefficients of a nonmagnetized plasma slab in one dimension. It was found that the JEC method has the same accuracy as the auxiliary differential equation (ADE) but possesses the same computational efficiency as the less accurate RC method. Numerical simulations showed that the JEC method exhibits significantly higher accuracy than the RC method in modeling wave attenuation inside the plasma.

APPENDIX A

NUMERICAL DERIVATION FOR \mathbf{J}

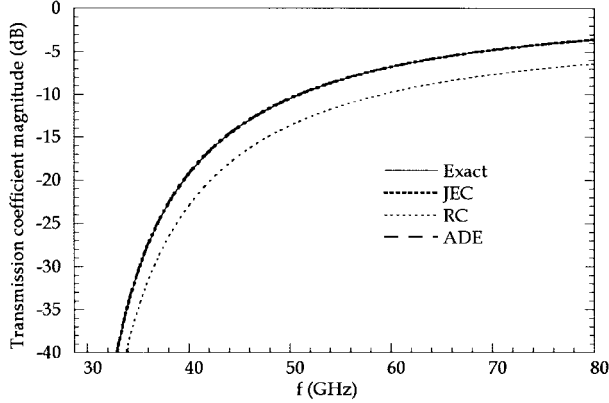
Rewriting (8)

$$\mathbf{J}(t) = \epsilon_0 \omega_{pe}^2 e^{-\nu_c t} \int_0^t e^{\nu_c \tau} \mathbf{E}(\tau) d\tau. \quad (\text{A.1})$$

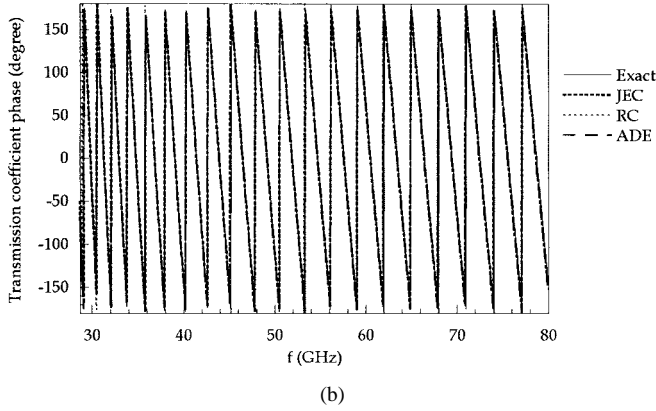
At the $n + 1/2$ and $n - 1/2$ moment of the i th point in a one-dimensional case

$$\begin{aligned} J_{yi}^{n+1/2} &= \epsilon_0 \omega_{pe}^2 e^{-\nu_c(n+1/2)\Delta t} \int_0^{(n+1/2)\Delta t} e^{\nu_c \tau} E_{yi}(\tau) d\tau \\ &= \epsilon_0 \omega_{pe}^2 e^{-\nu_c(n+1/2)\Delta t} \left(\int_0^{(n-1/2)\Delta t} e^{\nu_c \tau} E_{yi}(\tau) d\tau \right. \\ &\quad \left. + \int_{(n-1/2)\Delta t}^{(n+1/2)\Delta t} e^{\nu_c \tau} E_{yi}(\tau) d\tau \right) \end{aligned} \quad (\text{A.2})$$

$$\begin{aligned} J_{yi}^{n-1/2} &= \epsilon_0 \omega_{pe}^2 e^{-\nu_c(n-1/2)\Delta t} \int_0^{(n-1/2)\Delta t} e^{\nu_c \tau} E_{yi}(\tau) d\tau \end{aligned} \quad (\text{A.3})$$



(a)



(b)

Fig. 3. (a) Transmission coefficient magnitude for $V_c = 20 \times 10^9$ rad/s computed using the JEC, RC, and ADE methods. (b) Transmission coefficient phase computed using the JEC, RC, and ADE methods.

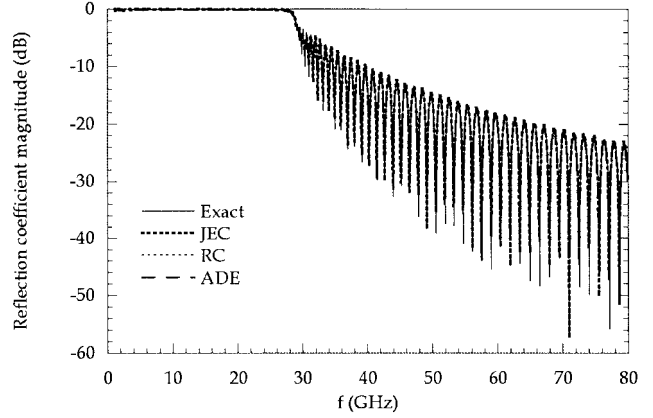
$$\begin{aligned}
 & e^{-\nu_c \Delta t} J_{yi}^{n-1/2} \\
 &= \varepsilon_0 \omega_{pe}^2 e^{-\nu_c (n+1/2) \Delta t} \int_0^{(n-1/2) \Delta t} e^{\nu_c \tau} E_{yi}(\tau) d\tau \quad (\text{A.4}) \\
 J_{yi}^{n+1/2} \\
 &= e^{-\nu_c \Delta t} J_{yi}^{n-1/2} + \varepsilon_0 \omega_{pe}^2 e^{-\nu_c (n+1/2) \Delta t} \int_{(n-1/2) \Delta t}^{(n+1/2) \Delta t} \\
 & \quad \cdot e^{\nu_c \tau} E_{yi}(\tau) d\tau. \quad (\text{A.5})
 \end{aligned}$$

Assuming,

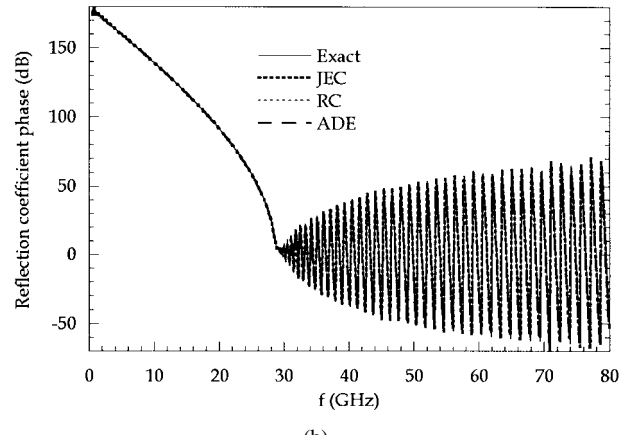
$$f(t) = e^{\nu_c t} E_{yi}(t). \quad (\text{A.6})$$

The central approximation of integration expansion can be written as

$$\begin{aligned}
 & \int_{(n-1/2) \Delta t}^{(n+1/2) \Delta t} e^{\nu_c \tau} E_{yi}(\tau) d\tau \\
 &= \int_{(n-1/2) \Delta t}^{(n+1/2) \Delta t} \left[f(n \Delta t) + f(n \Delta t)(\tau - n \Delta t) \right. \\
 & \quad \left. + f(n \Delta t) \frac{(\tau - n \Delta t)^2}{2} + O(\Delta t^3) \right] d\tau \\
 &= f(n \Delta t) \Delta t + 0 + f(n \Delta t) \frac{\Delta t^3}{24} + O(\Delta t^4) \\
 &= f(n \Delta t) \Delta t + O(\Delta t^3) \\
 &= e^{\nu_c n \Delta t} E_{yi}^n \Delta t + O(\Delta t^3). \quad (\text{A.7})
 \end{aligned}$$



(a)



(b)

Fig. 4. (a) Reflection coefficient magnitude for $V_c = 2 \times 10^9$ rad/s computed using the JEC, RC, and ADE methods versus frequency. (b) Reflection coefficient phase computed using the JEC, RC, and ADE methods versus frequency.

$J_{yi}^{n+1/2}$ becomes a second-order accurate approximation, (A.5) becomes

$$J_{yi}^{n+1/2} = e^{-\nu_c \Delta t} J_{yi}^{n-1/2} + \varepsilon_0 \omega_{pe}^2 e^{-\nu_c \Delta t/2} E_{yi}^n \Delta t. \quad (\text{A.8})$$

APPENDIX B JEC FORMULATIONS FOR DEBYE RELAXATION

According to the frequency-domain relations of the Debye relaxation

$$\varepsilon(\omega) = \varepsilon_0 \left(\varepsilon_\infty + \frac{\varepsilon_s - \varepsilon_\infty}{1 + j\omega t_0} \right) = \varepsilon_0 (\varepsilon_\infty + \chi(\omega)) \quad (\text{B.1})$$

where ε_s is the relative permittivity at dc, ε_∞ is the relative permittivity at $\omega = \infty$, and t_0 is the Debye relaxation time constant, then

$$\sigma(\omega) = j\omega \varepsilon_0 \frac{\varepsilon_s - \varepsilon_\infty}{1 + j\omega t_0}. \quad (\text{B.2})$$

The time-domain relations can be

$$\chi(t) = \frac{\varepsilon_s - \varepsilon_\infty}{t_0} e^{-t/t_0} U(t) \quad (\text{B.3})$$

and

$$\sigma(t) = \varepsilon_0 \frac{\varepsilon_s - \varepsilon_\infty}{t_0} \left(\delta(t) - \frac{1}{t_0} e^{-t/t_0} U(t) \right). \quad (\text{B.4})$$

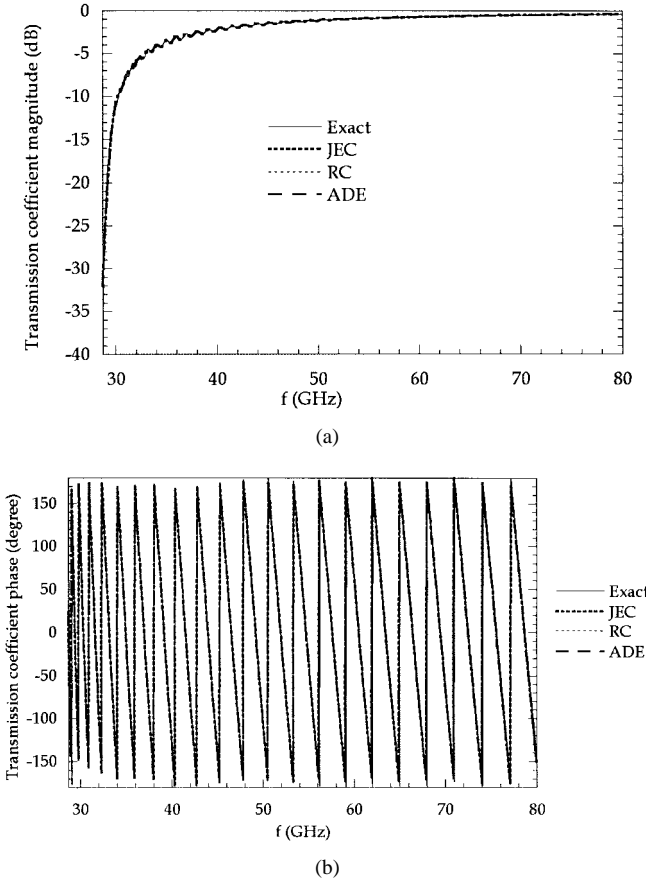


Fig. 5. (a) Transmission coefficient magnitude for $V_c = 2 \times 10^9$ rad/s computed using the JEC, RC, and ADE methods versus frequency. (b) Transmission coefficient phase computed using the JEC, RC, and ADE methods versus frequency.

From (21) and (22)

$$J(t) = \varepsilon_0 \frac{\partial}{\partial t} \int_0^t \chi(t-\tau) E(\tau) d\tau \quad (B.5)$$

or (8)

$$J(t) = \int_0^t \sigma(t-\tau) E(\tau) d\tau \quad (8)$$

we can obtain

$$J(t) = \varepsilon_0 \frac{\varepsilon_s - \varepsilon_\infty}{t_0} \left(E(t) - \frac{1}{t_0} e^{-t/t_0} \int_0^t e^{\tau/t_0} E(\tau) d\tau \right). \quad (B.6)$$

Using a similar approximation as the nonmagnetized plasma, $J^{n+1/2}$ can be approached as

$$\begin{aligned} J^{n+1/2} &= e^{-\Delta t/t_0} J^{n-1/2} + \varepsilon_0 \frac{\varepsilon_s - \varepsilon_\infty}{2t_0} \left(E^{n+1} + E^n \right. \\ &\quad \cdot \left(1 - e^{-\Delta t/t_0} - \frac{2}{t_0} e^{-\Delta t/(2t_0)} \right) \\ &\quad \left. - E^{n-1} e^{-\Delta t/t_0} \right) \end{aligned} \quad (B.7)$$

APPENDIX C JEC FORMULATIONS FOR LORENTZIAN RESONANCE

In the Lorentzian resonance medium, the frequency-domain relation is

$$\varepsilon(\omega) = \varepsilon_0 \left(\varepsilon_\infty + \frac{(\varepsilon_s - \varepsilon_\infty)\omega_0^2}{\omega_0^2 + 2j\omega\delta - \omega^2} \right) \quad (C.1)$$

where ω_0 is the resonant frequency, δ is the damping constant, ε_s is the relative permittivity at dc, ε_∞ is the relative permittivity at $\omega = \infty$. then

$$\sigma(\omega) = j\omega \varepsilon_0 \frac{(\varepsilon_s - \varepsilon_\infty)\omega_0^2}{\omega_0^2 + 2j\omega\delta - \omega^2} \quad (C.2)$$

and

$$\chi(\omega) = \frac{(\varepsilon_s - \varepsilon_\infty)\omega_0^2}{\omega_0^2 + 2j\omega\delta - \omega^2}. \quad (C.3)$$

Set

$$\alpha = \sqrt{\omega_0^2 - \delta^2}, \quad \cos \gamma = \frac{\delta}{\omega_0}, \quad \sin \gamma = \frac{\alpha}{\omega_0}$$

and

$$\beta = \frac{(\varepsilon_s - \varepsilon_\infty)\omega_0^2}{\sqrt{\omega_0^2 - \delta^2}} \quad (C.4)$$

$$\begin{aligned} \chi(t) &= \frac{(\varepsilon_s - \varepsilon_\infty)\omega_0^2}{\sqrt{\omega_0^2 - \delta^2}} e^{-\delta t} \sin \left(\sqrt{\omega_0^2 - \delta^2} t \right) U(t) \\ &= \beta e^{-\delta t} \sin(\alpha t) U(t) \end{aligned} \quad (C.5)$$

$$\sigma(t) = \varepsilon_0 \beta \omega_0 e^{-\delta t} \sin(\gamma - \alpha t) U(t). \quad (C.6)$$

According to (B.5) in the Lorentzian resonance medium, the current density in time can be derived as shown in (C.7), or according to (8), the current density can be directly derived from (C.6) as in (C.7) at the top of the next page and

$$\begin{aligned} J(t) &= \sigma(t) * E(t) \\ &= \varepsilon_0 \beta \omega_0 \int_0^t e^{-\delta(t-\tau)} \sin(\gamma - \alpha(t-\tau)) E(\tau) d\tau. \end{aligned} \quad (C.8)$$

For easy computation, we assume that

$$\begin{aligned} J(t) &= \text{Im}(j(t)) \\ &= \text{Im} \left(\varepsilon_0 \beta \omega_0 \int_0^t e^{-(\delta(t-\tau)+j(\gamma-\alpha t+\alpha\tau))} E(\tau) d\tau \right) \end{aligned} \quad (C.9)$$

$$\begin{aligned} j^{n+1/2} &= e^{-(\delta-j\alpha)\Delta t} j^{n-1/2} + \varepsilon_0 \beta \omega_0 e^{-j\gamma} \\ &\quad \cdot e^{-(\delta-j\alpha)\Delta t/2} E^n \end{aligned} \quad (C.10)$$

REFERENCES

- [1] K. S. Yee, "Numerical solution of initial boundary value problems involving Maxwell's equations in isotropic media," *IEEE Trans. Antennas Propagat.*, vol. 14, pp. 302-307, 1966.
- [2] A. Tafove and M. E. Brodwin, "Numerical solution of steady-state electromagnetic scattering problems using the time-dependent Maxwell's equations," *IEEE Trans. Microwave Theory Tech.*, vol. 23, pp. 623-630, 1975.
- [3] A. Tafove and K. R. Umashankar, "The finite-difference time-domain method for numerical modeling of electromagnetic wave interactions," *Electromagn.*, vol. 10, pp. 105-126, 1990.

$$\begin{aligned}
J(t) &= \varepsilon_0 \frac{\partial}{\partial t} (\chi(t) * E(t)) \\
&= \varepsilon_0 \beta \frac{\partial}{\partial t} \int_0^t e^{-\delta(t-\tau)} \sin \alpha(t-\tau) E(\tau) d\tau \\
&= \varepsilon_0 \beta \frac{\partial}{\partial t} \left[e^{-\delta t} \sin \alpha t \int_0^t e^{\delta \tau} \cos \alpha \tau E(\tau) d\tau - e^{-\delta t} \cos \alpha t \int_0^t e^{\delta \tau} \sin \alpha \tau E(\tau) d\tau \right] \\
&= \varepsilon_0 \beta \omega_0 e^{-\delta t} \left[(-\cos \gamma \sin \alpha t + \sin \gamma \cos \alpha t) \int_0^t e^{\delta \tau} \cos \alpha \tau E(\tau) d\tau + (\cos \gamma \cos \alpha t + \sin \gamma \sin \alpha t) \int_0^t e^{\delta \tau} \sin \alpha \tau E(\tau) d\tau \right] \\
&= \varepsilon_0 \beta \omega_0 e^{-\delta t} \left[\sin(\gamma - \alpha t) \int_0^t e^{\delta \tau} \cos \alpha \tau E(\tau) d\tau + \cos(\gamma - \alpha t) \int_0^t e^{\delta \tau} \sin \alpha \tau E(\tau) d\tau \right] \\
&= \varepsilon_0 \beta \omega_0 \int_0^t e^{-\delta(t-\tau)} \sin(\gamma - \alpha(t-\tau)) E(\tau) d\tau
\end{aligned} \tag{C.7}$$

[4] G. Mur, "Absorbing boundary conditions for finite-difference approximation of time-domain electromagnetic-field equation," *IEEE Trans. Electromagn. Compat.*, vol. 23, pp. 377–382, 1981.

[5] R. J. Luebbers, F. Hunsberger, and K. Kunz, "A frequency-dependent finite-difference time-domain formulation for transient propagation in plasma," *IEEE Trans. Antennas Propagat.*, vol. 39, pp. 29–34, 1991.

[6] R. J. Luebbers, F. Hunsberger, K. Kunz, and R. Standler, "A frequency-dependent finite difference time-domain formulation for dispersive materials," *IEEE Trans. Electromagn. Compat.*, vol. 32, pp. 22–227, 1990.

[7] K. Kunz and R. J. Luebbers, *The Finite-Difference Time-Domain Method for Electromagnetics*. Boca Raton, FL: CRC, 1993.

[8] R. J. Luebbers, D. Steich, and K. Kunz, "FDTD calculation of scattering from frequency-dependent materials," *IEEE Trans. Antennas Propagat.*, vol. 41, pp. 1249–1257, 1993.

[9] F. Hunsberger, R. J. Luebbers, and K. Kunz, "Finite-difference time-domain analysis of gyrotrropic media I: Magnetized plasma," *IEEE Trans. Antennas Propagat.*, vol. 40, pp. 1489–1495, 1992.

[10] R. J. Luebbers and F. Hunsberger, "FDTD for N th-order dispersive media," *IEEE Trans. Antennas Propagat.*, vol. 40, pp. 1297–1301, 1992.

[11] R. J. Hawkins and J. S. Kallman, "Linear electronic dispersion and finite-difference time-domain calculations: A simple approach," *J. Lightwave Technol.*, vol. 11, pp. 1872–1874, Nov. 1993.

[12] R. Siushansian and J. LoVetri, "A comparison of numerical techniques for modeling electromagnetic dispersive media," *IEEE Microwave Guided Wave Lett.*, vol. 5, pp. 426–428, 1995.

[13] D. F. Kelley and R. J. Luebbers, "Piecewise linear recursive convolution for dispersive media using FDTD," *IEEE Trans. Antennas Propagat.*, vol. 44, pp. 792–797, 1996.

[14] T. Kashiwa, N. Y. Yoshida, and I. Fukai, "Transient analysis of a magnetized plasma in three-dimensional space," *IEEE Trans. Antennas Propagat.*, vol. 36, pp. 1096–1105, 1988.

[15] T. Kashiwa and I. Fukai, "A treatment by FDTD method of dispersive characteristics associated with electronic polarization," *Microwave Opt. Technol. Lett.*, vol. 3, pp. 203–205, 1990.

[16] T. Kashiwa and I. Fukai, "A treatment by FDTD method of dispersive characteristics associated with orientation polarization," *IEEE Trans. Inst. Electron., Inform., Commun. Eng.*, vol. 73, pp. 1326–1328, 1990.

[17] M. D. Bui, S. S. Stuchly, and G. I. Costache, "Propagation of transients in dispersive dielectric media," *IEEE Trans. Microwave Theory Technol.*, vol. 39, pp. 1165–1171, 1991.

[18] R. M. Joseph, S. C. Hargness, and A. Taflove, "Direct time integration of Maxwell's equations in linear dispersive media with absorption for scattering and propagation of femtosecond electromagnetic pulse," *Opt. Lett.*, vol. 16, pp. 1412–1414, 1991.

[19] O. P. Gandhi, B.-Q. Gao, and T.-Y. Chen, "A frequency-dependent finite-difference time-domain formulation for general dispersive media," *IEEE Trans. Microwave Theory Technol.*, vol. 41, pp. 658–664, 1993.

[20] A. Taflove, *Computational Electrodynamics—The Finite-Difference Time-Domain Method*. Norwood, MA: Artech House, 1995.

[21] L. J. Nickisch and P. M. Franke, "Finite-difference time-domain solution of Maxwell's equations for the dispersive ionosphere," *IEEE Antennas Propagat. Mag.*, vol. 34, pp. 33–39, Oct. 1992.

[22] D. M. Sullivan, "Frequency-dependent FDTD methods using Z transforms," *IEEE Trans. Antennas Propagat.*, vol. 40, pp. 1223–1230, 1992.

[23] J. L. Young, "A full finite difference time domain implementation for radio wave propagation in a plasma," *Radio Sci.*, vol. 29, pp. 1513–1522, 1994.

[24] M. A. Lieberman and A. J. Lichtenberg, *Principles of Plasma Discharges and Materials Processing*. New York: Wiley, 1994.

[25] T. Sekiguchi, *The Principle of Modern Plasma*. Tokyo, Japan: Ohmu, 1979 (in Japanese).

[26] M. Tanaga and K. Nishigawa, *Physics of High Temperature Plasma*. Tokyo, Japan: Maruzen, 1991 (in Japanese).

[27] W. C. Chew, *Waves and Fields in Inhomogeneous Media*. New York: Van Nostrand Reinhold, 1990.



Qing Chen received the B.S. and M.S. degrees (electrical engineering—specializing in power systems) from Fuzhou University, China, in 1985 and 1988, respectively, and the Ph.D. degree from the University of Tokyo, Japan (electrical engineering), in 1997.

From 1988 to 1993, she worked as a Teaching Assistant and a Lecturer at Fuzhou University. During this time she engaged in the research and development of electrical switches using the finite-element method. She is presently a Visiting Researcher at the University of Tokyo. Her current research interests include the analysis of wave propagation inside plasmas and the study of plasma processing devices using the finite-difference time-domain method.



Makoto Katsurai was born in Kamakura City, Kanagawa Prefecture, Japan, on November 13, 1941. He received the Ph.D. degree in electrical engineering from the University of Tokyo, Japan, in 1970.

In 1970, he joined the Department of Electrical Engineering, University of Tokyo, where he is currently a Professor. In 1980, he was with the Princeton Plasma Physics Laboratory, Princeton, NJ, as a Visiting Research Fellow. His research interests include engineering applications of plasmas ranging from low-temperature processing plasmas to high-temperature fusion plasmas, particularly compact torus plasmas produced by the merging process.



Paul H. Aoyagi received the B.S. degree from the University of California, Davis, CA, in 1985 and the M.S. and Ph.D. degrees in electrical engineering from the University of Illinois, Urbana-Champaign, in 1988 and 1992, respectively, all in electrical engineering.

From 1992 to 1994, he was a Postdoctoral Researcher at the University of Tokyo, Japan. Since 1994 he has been with the Production Engineering Research Laboratory of Hitachi, Ltd., Yokohama, Japan, where he has been engaged in the modeling of simultaneous switching noise inside multichip modules power planes using both equivalent circuit modeling and the finite-difference time-domain method. He is currently involved in the research and development of electromagnetic interference countermeasures to reduce the radiation from computer packaging. His research interests include the mathematical error analysis of numerical methods and microwave theory.

Dr. Aoyagi was the recipient of an IBM fellowship (1990 to 1992) and the Japanese Ministry of Education scholarship (1992 to 1994).